Published in final edited form as:
Int J Comput Assist Radiol Surg. 2011 September ; 6(5): 617–626. doi:10.1007/s11548-010-0539-z.

Outcome quantification using SPHARM-PDM toolbox in orthognathic surgery

Beatriz Paniagua,
Department of Orthodontics, University of North Carolina at Chapel Hill, Chapel Hill, NC, USA

Lucia Cevidanes,
Department of Orthodontics, University of North Carolina at Chapel Hill, Chapel Hill, NC, USA

HongTu Zhu, and
Department of Biostatistics, University of North Carolina at Chapel Hill, Chapel Hill, NC, USA

Martin Styner
Department of Psychiatry and Computer Science, University of North Carolina at Chapel Hill, Chapel Hill, NC, USA

Beatriz Paniagua: beatriz_paniagua@dentistry.unc.edu; Lucia Cevidanes: cevidanl@dentistry.unc.edu; HongTu Zhu: hzhu@bios.unc.edu; Martin Styner: styner@cs.unc.edu

Abstract

Purpose—Quantification of surgical outcomes in longitudinal studies has led to significant progress in the treatment of dentofacial deformity, both by offering options to patients who might not otherwise have been recommended for treatment and by clarifying the selection of appropriate treatment methods. Most existing surgical treatments have not been assessed in a systematic way. This paper presents the quantification of surgical outcomes in orthognathic surgery via our localized shape analysis framework.

Methods—In our setting, planning and surgical simulation is performed using the surgery planning software CMFapp. We then employ the SPHARM-PDM to measure the difference between pre-surgery and virtually simulated post-surgery models. This SPHARM-PDM shape framework is validated for use with craniofacial structures via simulating known 3D surgical changes within CMFapp.

Results—Our results show that SPHARM-PDM analysis accurately measures surgical displacements, compared with known displacement values. Visualization of color maps of virtually simulated surgical displacements describe corresponding surface distances that precisely describe location of changes, and difference vectors indicate directionality and magnitude of changes.

Conclusions—SPHARM-PDM-based quantification of surgical outcome is feasible. When compared to prior solutions, our method has the potential to make the surgical planning process more flexible, increase the level of detail and accuracy of the plan, yield higher operative precision and control and enhance the follow-up and documentation of clinical cases.

Keywords

Orthognathic surgery; Surgical outcome; SPHARM-PDM; Statistical shape analysis

Correspondence to: Beatriz Paniagua, beatriz_paniagua@dentistry.unc.edu.

Conflict of interest None.

Introduction

Craniofacial deformity occurs in around 5% of the US population, and 1–2% have a deformity severe enough to be disabling and stigmatizing. Individuals with craniofacial deformities experience speech and masticatory problems as a result of their condition [4,22]. They may also be alienated, socially stereotyped or otherwise mistreated by their peers because of their appearance, leading to psychosocial stress [21,23]. Currently, assessment of correction of skeletal discrepancies is based on visual data originating from different sources: clinical examination, 3D photographic examination, Cone-Beam Computed Tomography (CBCT) and digital dental models. Correction of these deformities using orthognathic surgery involves careful repositioning the jaws, due to the unique features of each patient's deformity. Conventional methods to evaluate treatment for orthognathic surgery still rely on 2D lateral and frontal radiographic images, although several researchers [15] have highlighted the importance of 3D analysis for dental applications, similar to the ones proposed in this paper. Surgical jaw displacements are 3D movements in space, and 2D measurements cannot assess 3D rotational axes. For example, in 2D lateral X-rays, the left and right structures overlap, which severely limits the quantification of these components as separate surfaces for asymmetrical surgical correction. Therefore, 2D diagnostic procedures are often of limited help for the understanding of complex three-dimensional defects and for the planning of appropriate corrections. Even though 3D CBCT images are now easily obtained in many dental centers, the ability to visualize the craniofacial complex in 3D does not imply the ability to quantify growth or treatment changes in 3D. This paper discusses methods for quantification of jaw surgery outcome. To quantify surgical changes of known amounts, surgery simulation is performed by using an extensive computer-aided surgery (CAS) system for orthognathic surgery called CMF application software (CMFapp [9–13,18]) developed M.E. Müller Institute for Surgical Technology and Biomechanics, University of Bern, Switzerland, under the funding of the Co-Me network, http://co-me.ch and available to us under a collaborative agreement. Using the SPHARM-PDM shape analysis toolbox [24,25], we aim to improve the ability to measure jaw displacements and bone remodeling post-surgery for correction of craniofacial deformities. SPHARM-PDM toolbox presents a comprehensive set of tools for the computation of 3D structural statistical shape analysis. In summary, the SPHARM description is a hierarchical, global, multi-scale boundary description that can only represent objects of spherical topology, proposed initially by [5]. This SPHARM shape analysis approach was extended by [16,17] to use the implied sampled surface (SPHARM-PDM, where PDM stands for Point Distribution Models). It has been applied in several studies on brain morphometry, but can potentially be employed in other 3D shape problems. This framework [25] was developed as part of the National Alliance of Medical Image Computing, (NAMIC, NIH Roadmap for Medical Research) and has been adapted for use with cone-beam CTs of the craniofacial complex. This work presents an improvement in outcome measurement when compared to previous closest point correspondence (CP)-based analysis [6,19]. This standard CP analysis is a brute force algorithm that calculates a vertex to vertex Euclidean closest point distance, and it is currently used by most commercial and academic softwares, but does not map corresponding surfaces based in anatomical geometry, and thus, it usually underestimates rotational and large translational movements. Moreover, CP measures surgical jaw displacement as the smallest separation between boundaries of the same structure that may not be the right anatomical corresponding boundaries on pre- and post-surgery anatomical structures. Therefore, it is the aim of this paper to validate shape analysis methods for quantification of surgical outcomes in orthognathic surgery, using virtually simulated surgical models. To this end, the paper is structured as follows: in "Methods" the methodological framework is described, consisting in: image acquisition and segmentation ("Image acquisition and segmentation"), 3D diagnosis (in "3D diagnosis") and CAS framework used to simulate surgical procedures ("SPHARM-PDM for orthognathic

surgery"). "Results" describes the results obtained in the quantification of the virtual surgery outcomes, while "Discussion" has the conclusion and discussion points.

Methods

For the research presented in this paper, an existing dataset of pre-surgery CBCT images from 20 patients enrolled in the study *Influences on Stability following Orthognathic Surgery* (NIDCR DE005215) are used. Institutional review board approval and informed consent were obtained for all subjects. Fourteen patients who had combined maxillary advancement and mandibular setback surgery and 6 patients who had 1-piece maxillary advancement surgery were selected (11 women and 9 men, 20 in total).

Image acquisition and segmentation

Cone-beam CT (CBCT)images are acquired before surgery and at splint removal (4–6 weeks postsurgery) with the New-Tom 3G (AFP Imaging, Elmsford, NY). The imaging protocol involves a 36-second head CBCT scan with a 12-in field of view. All CBCT scans are acquired with the patient biting on a thin wax bite to maintain centric occlusion [26]. The next step in our processing pipeline is image segmentation, where the anatomical structures of interest are identified and delineated in the CBCT image. In orthognathic surgery, the goal of segmentation is to obtain a 3D representation (surface model) of the hard tissue that is usable for virtual planning. Currently available 3D image analysis software tools offer many manual, semi-automatic and fully automatic segmentation techniques (Dolphin, 3DMD Vultus and Maxilim). Automatic segmentation does not offer the best results for virtual surgery planning, since the condyles, the internal surface of the ramus and maxilla are not segmented correctly using automatic procedures. For this research and in order to best capture the above mentioned and other areas of choice, we use the semi-automatic segmentation procedures provided by the ITK-SNAP [29] open-source software followed by manual post-processing. The automatic segmentation procedures in ITK-SNAP utilize active contour methods to compute feature images based on the CBCT image gray level intensity and boundaries with a voxel dimension of $0.5 \times 0.5 \times 0.5$ mm. After obtaining the segmentation result, manual post-processing is necessary to remove common artifacts resulting from metallic elements. Lower and upper jaws are usually connected due to insufficient image resolution and must be separated within the temporomandibular joint (TMJ) and on occlusal surfaces in particular. Currently, the manual post-processing step is too time-consuming and not practical for the surgeon. Further research in advanced segmentation methods for this application field is essential to reach the ideal of an accurate and continuous individual segmentation of the skeletal base, obtained with only a few mouse clicks. After segmentation of the anatomical structures of interest, ITK-SNAP allows a 3D display of the anatomical areas directly from the volume data.

3D diagnosis

3D diagnosis and treatment planning is performed using CMFapp, so that simulated changes represent surgical procedure movements that are clinically meaningful, rather than rotations and translations of the mandible that would not be clinically meaningful. Therefore and following segmentation, the 3D surface models are visualized and manipulated in CMFapp that provides several tools to properly diagnose skeletal discrepancies and malocclusions:

- *3D Cephalometry* is performed on the 3D skeletal models generated from CBCT, defining landmarks, lines, planes and measurements. This approach highly improves classical clinical cephalometric analyses that have been based on a set of points, either of anatomical meaning or from an abstract definition (such as middle point between two other points) from 2D radiographs. Surface and shape data

available in 3D imaging provide new characterization schemes, based on higher order mathematical entities (e.g., spline curves and surfaces).

- *Mirroring* can be a valuable technique in the treatment of asymmetries. The CAS software used in this study has the capability of computing asymmetry-related measurements that are indeed useful tools for the 3D diagnosis and preparation of the surgical plan [2]. However, the patient sample presented in this study did not have facial asymmetry, so detailed description of mirroring techniques will be a topic for future studies that include asymmetric patients.

Surgical planning and simulation

After diagnosis, the next step is to use 3D virtual surface models to plan and simulate the surgical intervention using CMFapp. For each clinical case, simulated surgery outcomes are created and compared with the imaging data acquired prior surgery (Fig. 1). The surgical correction of craniofacial deformity and the assessment of growth and treatment outcomes require precise quantification of the 3D displacements [3,7,8]. CMFapp is used to perform the virtual cuts and displacements that are then matched with planned clinical osteotomy segments. The quantitative displacements between pre-surgery and simulated surgery are finally measured via the SPHARM-PDM shape framework that employs shape-based correspondence. The surgical simulation steps include [28],

- *Simulation of surgical osteotomy cuts.* Simulated surgeries are performed on the 3D pre-surgery models by a single examiner using CMFapp. The osteotomy cuts for a standard bilateral split osteotomy (BSSO) and maxillary Le Fort I osteotomy are executed by placing points on the pre-surgery models at the area and in the orientation of the osteotomy cuts. The locations of surgical osteotomy cuts are determined by the anatomic characteristics of each patient, such as thickness of the mandibular ramus, position of the mandibular canal and proximity to the roots of the second molars. The osteotomy cuts then determine 4 surgical segments for the mandible (right ramus, left ramus, mandibular body and chin) and 1 piece for maxilla (Fig. 2).
- *Simulation of surgical displacements.* The magnitude and direction of the simulated movements are planned by the 3D diagnosis. Movements for each surgical piece were performed allowing six degrees of freedom (3 translational parameters: anteriorposterior, lateral, superiorinferior; and 3 rotational parameters: yaw, pitch and roll). Pre-surgery 3D models for each subject are displaced virtually with known 3D surgical displacements.

SPHARM-PDM for orthognathic surgery

The six degrees of freedom [1] (DOF) of jaw movements for surgical osteotomy cuts (3 translation axes and 3 rotation axes) cannot be appropriately measured with 2D X-rays or by the standard 3D closest point (CP)-based analysis. Correspondence established by means of CP methods is usually bad, since topology or geometrical structure of the surfaces is not taken into account; therefore, measured 6 DOF are expected not to be accurately measured. Unlike 3D CP methods, the shape-based SPHARM-PDM correspondence is able to accurately identify and quantify critical attributes of the surgical correction, such as the rotational axes of bone displacements and remodeling.

For these reasons, SPHARM-PDM UNC shape toolbox was employed to provide a unique quantitative assessment by computing correspondent 3D models of pre-surgery and simulated surgery surfaces for each surgical segment.

Segment Pre-processing—Before computing the SPHARM-PDM shape correspondence, spherical topology of the anatomical segments must be assured, which is achieved with a few pre-processing steps. First, the virtual osteotomy cuts in CMFapp (Fig. 3b) leave open surgical segments that need to be closed to preserve spherical topology needed to use SPHARM-PDM shape analysis Toolbox (Fig. 3c). Second, in order to antialias the ridges and waves of the segments, a smoothing procedure was applied (Fig. 3d). In the last pre-processing step, a binary segmentation volume is created from the surfaces. This was done via finding the enclosing bounding box of the shape and binarizing the cross-sections. These binary segmentation volumes (Fig. 3e) are the input of the SPHARM-PDM framework.

Point-based Model Computing—The input of SPHARM-PDM is a set of binary pre-processed surgical segment volumes. These segmentations are first processed to ensure spherical topology and then converted to surface meshes. Next, the spherical parametrization is computed from the surface meshes using an area-preserving, distortion minimizing spherical mapping. The SPHARM description is computed from the mesh and its spherical parametrization [25]. This description is then sampled into a triangulated surfaces (SPHARM-PDM) via a icosahedron subdivision of the spherical parametrization (Fig. 4). Alignment of triangulated surfaces was not performed in order to quantify the degree of rotation and translation between the presurgical segments and those after surgical simulation (Fig. 3f). In our experience, the sampling for the mandibular and maxillary structures should be chosen between subdivision level 20 (4002 surface points) and 30 (9002 surface points) depending on the complexity of the objects. For this study, we selected subdivision 20 since we believe that there will be a minimum issue with accuracy since we only have to capture 6 DOF. SPHARM degree that offered the lowest reconstruction errors and therefore used for this study is 16.

Measurement of surgical outcomes

A preliminary analysis is computed by subtracting pre- and simulated surgery models and displayed via color-coded distance magnitude and vector maps. The distance maps display the magnitude of the pose changes between pre-surgery and virtual post-surgery point-based models (Fig. 3g, green shows no changes, red shows the maximum changes). Vector maps provide visualization of displacements between paired correspondent point-based models, indicating the direction and magnitude of displacements (i.e. expansion or contraction might be shown depending on the direction of the vectors, Fig. 3h). However, further analysis is needed to capture translation and rotation information. These translation and rotation parameters are estimated via a rigid Procrustes alignment procedure. This rigid Procrustes alignment procedure computes an optimal linear, geometric transformation $\varphi(n)$ that best maps the shape changes between pre-surgery and virtual post-surgery models based on the established correspondence.

Statistical evaluation

The differences between six known DOF rotation and translation parameters from the simulated surgery plan and the values obtained with Procrustes alignment of the SPHARM-PDM models were computed:

$\bar{d}_{j,Rot} = \sum_{i=1}^{n} |DOFRot_{i,j}^{simul} - DOFRot_{i,j}^{procrustes}|/n$ and
$\bar{d}_{j,Tra} = \sum_{i=1}^{n} |DOFTra_{i,j}^{simul} - DOFTra_{i,j}^{procrustes}|/n$ for j = 1, 2, 3 which each j denotes a specific DOF parameter of rotation and translation. The results given in Table 1 are all based on the difference metric $\bar{d}_j$. Three statistical measures used to quantify these differences include (1) $P(|\bar{d}_{j,Tra}| < 0.5)$ or $P(|\bar{d}_{j,Rot}| < 5)$ for average translation in mm or for average rotation in

degrees, (2) 95% confidence interval (CI) for $\bar{d}_{j,Rot}$ and $\bar{d}_{j,Tra}$ and (3) 95% prediction interval (PI) for $\bar{d}_{j,Rot}$ and $\bar{d}_{j,Tra}$. Each of these measures is described as follows:

1. $P(|\bar{d}_{j,Tra}| < 0.5)$ (or $P(|\bar{d}_{j,Rot}| < 5)$) is the probability that the sample mean difference $\bar{d}_{j,Rot}$ (or $\bar{d}_{j,Tra}$) is less than 0.5 mm for translation in mm (or 5 degrees for rotation). Here, 0.5 mm is the image spatial resolution for translation, and 5 degrees for rotation was chosen to represent the maximum rotation error that we want to achieve.

2. 95% confidence interval (CI) is an interval that covers the true mean of $\bar{d}_{j,Rot}$ (or $\bar{d}_{j,Tra}$) with 95% confidence. Let $\bar{d}_j$ be either $\bar{d}_{j,Rot}$ or $\bar{d}_{j,Tra}$. The CI was calculated as $\bar{d}_j \pm t_{(0.025,n-1)} \frac{s_{d,j}}{\sqrt{n}}$, where $s_{d,j}$ is the standard deviation based on the calculated differences for DOF parameters, and $t_{(0.025,\ n-1)}$ is the 0.025 critical value of the *t*-distribution with $df = n - 1$. Thus, a 95% CI containing ±0.5 for translation parameters (or ±0.5 for rotation parameters) represents a large degree of concordance between the known displacements and the measured displacements using SPHARM-PDM analysis on average.

3. 95% prediction interval (PI) is an interval that a future observation $P(|\bar{d}_{j,\ Tra}| < 0.5)$ (or $P(|\bar{d}_{j,\ Rot}| < 5)$) will fall in with 95% probability. It is a confidence interval for prediction. 95% PI can be computed by $\bar{d}_j \pm t_{(0.025,n_d-1)} s_{d,j} \sqrt{1+\frac{1}{n}}$. The prediction interval can quantify the size of the DOF parameter difference at the individual level, whereas the first two measures only allow us to measure the average DOF parameter difference. Thus, a 95% PI containing ±0.5 for translation parameters (or ±5 for rotation parameters) represents a large degree of concordance between the known displacements and the measured displacements using SPHARM-PDM analysis.

Finally, the paired two-sample T^2 test was used to statistically test the null hypothesis that there is no difference between the known displacements and the measured displacements using SPHARM-PDM analysis.

Results

The results are given in Table 1 for each surgical segment grouping and Table 2 for all surgical segments grouping. Each table presents mean differences 95% CIs and 95% PIs for quantification of surgical displacements, for all three degrees rotations and three degrees translations. Statistical analysis results in Table 1 revealed very high probability (ranging 0.99–1) that the difference between the real rotation and the measured rotation was less than 5 degrees for all the segments. In case of the translations, very high probabilities also were found that the difference between the real translation and the measured one was less than 0.5 mm (image spatial resolution), except in case of the chin that has lower probabilities (ranging 0.75–0.99). However, all cases for rotation and translation measurements showed >0.7 probability, which is still high probability. The 95% CI tests contained the hyphotesized means ($\bar{X}_{\text{diffTrans}} = 0$ or $\bar{X}_{\text{diffRot}} = 0$) both in Tables 1 and 2. All the 95% PI intervals for all the different segments contained the hyphotesized means (Observe that PI is wider than CI, see Table 1). In the Table 2, all obtained values for $P(|\bar{d}_{jtra}| < 0.5)$*or* $P(|\bar{d}_{jrot}| < 5)$ were 1, showing that all the measured displacements would be within 0.5 mm of translation and 5 degrees of rotation of the real displacement. All 6 DOF for 95% CI and 95% PI contain 0, so in general, it is pretty certain that the null hypothesis $H_0 : \mu_d = 0$ is fulfilled by our data. The results offered for all surgical segments grouped show even better results, with high probabilities of having measured differences of less than 0.5 mm of translation and less than 5 degrees of rotation. All PI and CI intervals contained the hyphotesized means. Finally, except for two DOF parameters of Maxillary Body, the known

displacements did not differ significantly from the measured displacements using SPHARM-PDM analysis at a level of 5%. Even for these two DOF parameters of Maxillary Body, the significances were marginal (Maxillary Body translation in *Y*-plane *t*-value = 3.7 and associated *p*-value = 0.0015 and Maxillary Body rotation in the *Z*-plane *t*-value = −2.76 and associated *p*-value = 0.01).

Discussion

This pilot study reveals the suitability of SPHARM-PDM UNC Shape Correspondence toolbox to accurately measure surgical outcomes in orthognathic surgeries. Three-dimensional diagnosis and treatment planning, combined with 3D shape analysis, have great potential for future benefit to patients and surgeons, as a complement to the current diagnostic procedures used in clinical environment. In this paper, virtual surgery generated with CMFapp accurately recreated all surgical movements in three rotational and three translational planes of space. After 3D shape analysis, all the measurements were within a range of 0.5 mm of translation and 5 degrees of rotation of the known surgical displacements. This is considered to be an adequate precision for the proposed clinical application.

The SPHARM-PDM results presented in this paper show enhanced outcome measures over a CP-based analysis (see Fig. 5) offering not only quantitative displacement values for each anatomic region, but also providing tools that give a sense of directionality of the displacements (Fig. 6). In addition, CP measurement methods have been applied previously to measure surgical outcomes [6–8,19,28]. Only 2 of the measured differences between known values and SPHARM-PDM pre- and post-surgery models were greater than 1 mm. All differences were less than 0.5 mm and 0.75 degrees. Differences less than 2 mm are considered to be clinically non-significant [14,20,27].

The techniques in this paper resulted in an evaluation of the quantification of surgical outcomes using SPHARM-PDM, allowing assessment and visual display of the location and direction changes, and magnitude of agreement between known values of simulation and measurements of displacements with SPHARM-PDM. Computer-assisted surgical simulation allowed manipulation of the images in the necessary 6 degrees of freedom to accurately reproduce the actual surgical outcome.

In recent years, there has been an explosion of commercially available software tools for 3D visualization. The biggest drawback of these tools is the lack of validation of the surgical outcome quantification. For clinical applicability, it is necessary that the quantification of craniofacial skeletal components, occlusion and soft tissue changes are validated. This article demonstrated that SPHARM-PDM software can correctly quantify surgical changes in craniofacial skeletal components of patients. Our future studies will apply these same methods to extensive longitudinal datasets of orthognathic surgery in order to measure post-surgical changes and adaptation after splint removal, after 1 year, and after 3 years, when compared with the pre-surgery data.

Acknowledgments

Funding provided by NIDCR DE018962, NA-MIC NIH U54 EB005149.

References

1. Ackerman J, Proffit W, Sarver D, Ackerman M, Kean M. Pitch, roll, and yaw: describing the spatial orientation of dentofacial traits. Am J Orthod Dentofacial Orthop. 2007; 3(123):305–310. [PubMed: 17346584]

2. Alhadidi A, Cevidanes L, Mol A, Ludlow J, Styner M. 3d analysis of facial asymmetry based on midsaggital plane computation. J Dent Res. 2009; 1(88):311.
3. Bailey L, Cevidanes L, Proffit W. Stability and predictability of orthognathic surgery. Am J Orthod Dentofacial Orthop. 2004; 1(126):273–277. [PubMed: 15356484]
4. Beals S, Joganic E. Form and function in craniofacial deformities. Semin Pediatr Neurol. 2004; 4(11):238–242. [PubMed: 15828706]
5. Brechbuhler C, Gerig G, Kubler O. of closed surfaces for 3-D shape description. Comput Vis Graph Image Process. 1995; 61(1):154–170.
6. Carvalho F, Cevidanes L, Motta A, MA A, Phillips C. 3d assessment of mandibular advancement 1 year after surgery. Am J Orthod Dentofacial Orthop. 2010; 1(1) Accepted.
7. Cevidanes L, Oliveira C, Phillips C, Motta A, Styner M, Tyndall D. Three dimensional short-term mandibular displacements following class iii surgery. J Dent Res. 2006; 1(86):1827–1831.
8. Cevidanes, L.; Styner, M.; Phillips, C.; Oliveira, A.; Tulloch, J. 3d morphometric changes 1 year after jaw surgery. Biomedical imaging: macro to nano IEEE international symposium; 2007. p. 1332-1335.
9. Chapuis, J. PhD thesis. University of Bern; 2006. Computer-aided cranio-maxillofacial surgery.
10. Chapuis, J.; Langlotz, F.; Blaeuer, M.; Hallermann, W.; Schramm, A.; Caversaccio, M. A novel approach for computer-aided corrective jaw surgery. 3rd international conference on computer-aided surgery around the head; 2005a.
11. Chapuis J, Ryan P, Blaeuer M, Langlotz F, Hallermann W, Schramm A. A new approach for 3d computer-assisted orthognathic surgery—first clinical case. Comput Assist Radiol Surg. 2005b
12. Chapuis J, Schramm A, Pappas I, Hallermann W, Schwenzer-Zimmerer K, Langlotz F. A new system for computer-aided preoperative planning and intraoperative navigation during corrective jaw surgery. IEEE Trans Inf Technol Biomed. 2007; 1(22):274–287. [PubMed: 17521077]
13. DeMomi E, Chapuis J, Pappas I, Ferrigno G, Hallermann W, Schramm A. Automatic extraction of the mid-facial plane for cranio-maxillofacial surgery planning. Int J Oral Maxillofac Surg. 2006; 1(35):636–642.
14. Donatsky O, Hillerup S, Bjorn-Jorgensen J, Jacobsen PU. Computerized cephalometric evaluation of orthognathic surgical precision and stability in relation to maxillary superior repositioningcombined with mandibular advancement or setback. Int J Oral Maxillofac Surg. 1997; 21(1992):199–203. [PubMed: 1402047]
15. Farman A. Oral and maxillofacial radiology: the allegory of the cave revisited. Oral Surg Oral Med Oral Pathol Oral Radiol Endod. 2008; 105(2):133–135. [PubMed: 18230383]
16. Gerig, G.; Styner, M.; Shenton, ME.; Lieberman, JA. Shape versus size: improved understanding of the morphology of brain structures. International conference on medical image computing and computer assisted intervention; 2001; MICCAI; 2001. p. 24-32.
17. Gerig G, Styner M, Jones D, Weinberger D, Lieberman JA. Shape analysis of brain ventricles using spharm. Math Methods Biomed Image Anal MMBIA. 2001; (2001):171–178.
18. Krol Z, Chapuis J, Schwenzer-Zimmerer K, Langlotz F, Zeilhofer H. Preoperative planning and intraoperative navigation in the reconstructive craniofacial surgery. J Med Infor Technol. 2005; 1(9):83–89.
19. Motta A, Cevidanes L, Carvalho F, Almeida M, Phillips C. 3d regional displacements after mandibular advancement surgery: a 1-year follow-up. Int J Oral Maxill Surg. 2010; 1(1) Accepted.
20. Ong T, Banks R, Hildreth A. Surgical accuracy in le fort i maxillary osteotomies. Br J Oral Maxill Surg. 2001; 2(39):96–102.
21. Phillips C, Bennett M, Broder H. Dentofacial disharmony: psychological status of patients seeking treatment consultation. Angle Orthod. 1998; 1(68):547–556. [PubMed: 9851353]
22. Proffit W, Fields H, Moray L. Prevalence of malocclusion and orthodontic treatment need in the united states: estimates from the n-hanes iii survey. Int Adult Orthodon Orthognath Surg. 1998; 1(13):97–106.
23. Rankin M, Borah G. Perceived functional impact of abnormal facial appearance. Plast Reconstr Surg. 2003; 7(111):2147–2148.

24. Styner M, Lieberman JA, McClure RK, Weinberger DR, Jones DW, Gerig G. Morphometric analysis of lateral ventricles in schizophrenia and healthy controls regarding genetic and disease-specific factors. Proc Natl Acad Sci USA. 2005; 102(13):4872–4877. [PubMed: 15772166]

25. Styner, M.; Oguz, I.; Xu1, S.; Brechbuhler, C.; Pantazis, D.; Levitt, J.; Shenton, M.; Gerig, G. Framework for the statistical shape analysis of brain structures using spharm-pdm. Insight J. 2006 [Accessed 9th Nov]. http://www.insightjournal.org/

26. Swennen GR, Mollemans W, De Clercq C, Abeloos J, Lamoral P, Lippens F. A cone-beam computed tomography triple scan procedure to obtain a three-dimensional augmented virtual skull model appropriate for orthognathic surgery planning. J Craniofac Surg. 2009; 20(2):297–307. [PubMed: 19276829]

27. Tng T, Chan T, Hgg U, Cooke M. Validity of cephalometric landmarks. An experimental study on human skulls. Eur J Orthod. 1994; 2(16):110–120. [PubMed: 8005198]

28. Tucker S, Cevidanes L, Styner M, Kim H, Reyes M, Proffit W, Turvey T. Comparison of actual surgical outcomes and 3d surgical simulations. International Journal of Oral and Maxillofacial Surgery. 2009; 1(1) Accepted.

29. Yushkevich P, Piven J, Hazlett H, Smith R, Ho S, Gee J. User-guided 3d active contour segmentation of anatomical structures: significantly improved efficiency and reliability. Neuroimage. 2006; 1(31):1116–1128. [PubMed: 16545965]

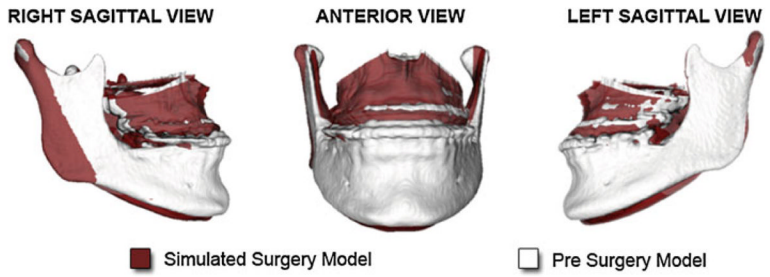

Fig. 1.
Semi-transparent overlay 3D model (*red*) of the projected surgical plan, over the pre-surgery (*white*) 3D model

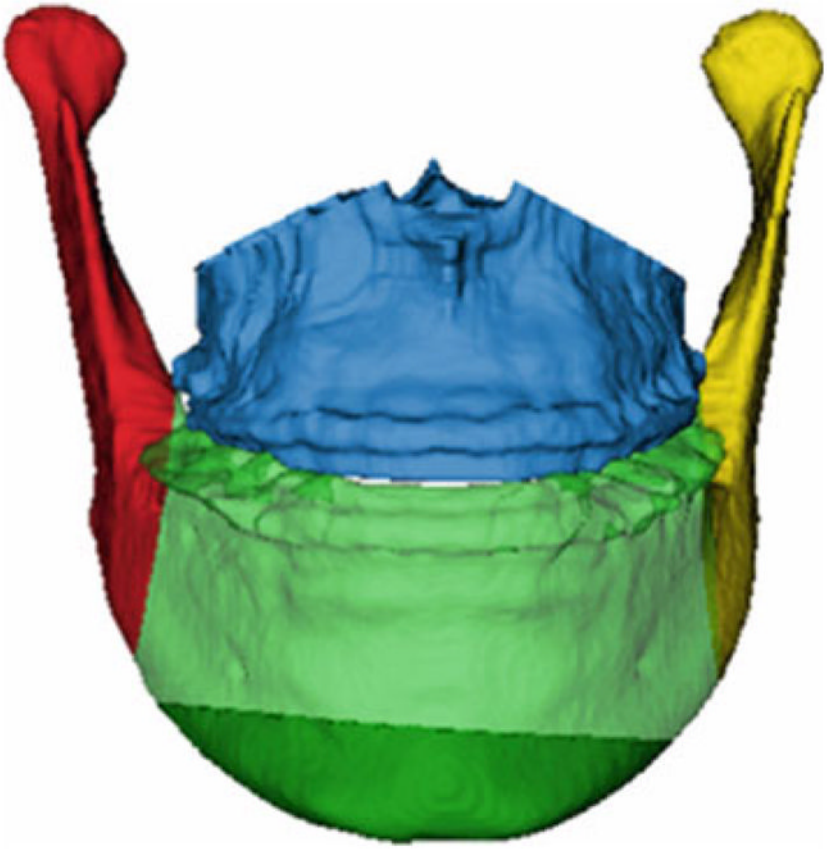

Fig. 2.
Example of surgical cuts in a corrective surgical procedure. Depending on the surgical plan, up to 5 segments are planned for each patient: *chin* (*dark green*), *left ramus* (*yellow*), *right ramus* (*red*), *mandibular body* (*light green*) and *maxillary body* (*blue*)

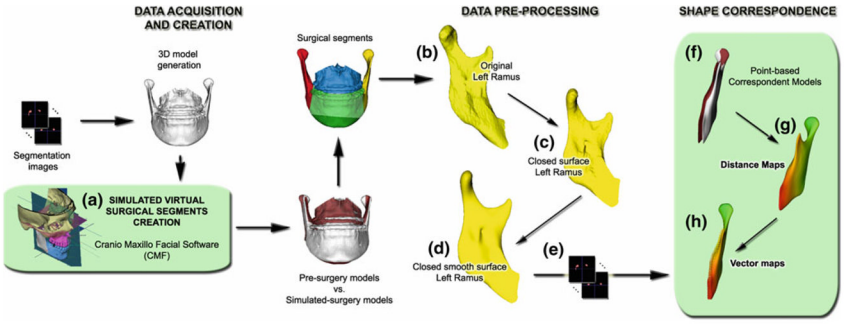

Fig. 3.

Shape Correspondence designed pre-processing pipeline. After image acquisition, segmentation and diagnosis surgical plan is designed (**a**), and surgical segments are generated by virtual surgical osteotomy cuts (**b**). Data are preprocessed next, by closure of open osteotomies sites (**c**), and smoothing (**d**). Surface information is scan converted back to binary volumes (**e**), and correspondence is established (**f**). Visualization of surgical displacement is possible by means of distance maps (**g**) and vector maps (**h**)

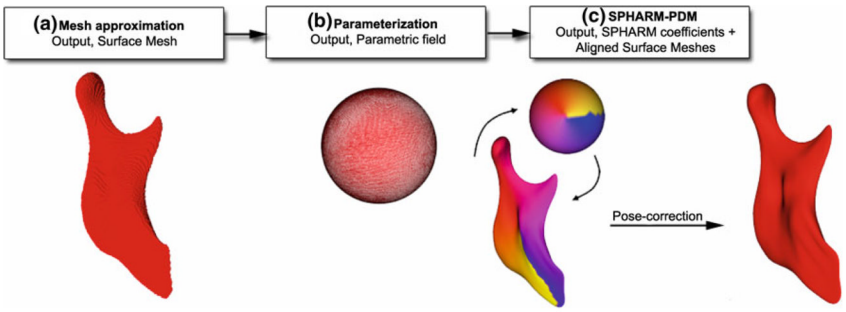

Fig. 4.

Surface models of each of the surgical segments are converted into surface meshes (**a**), and spherical parameterization is computed (**b**). Using the first-order ellipsoid from SPHARM coefficients, spherical parameterizations establish correspondence across surfaces (**c**)

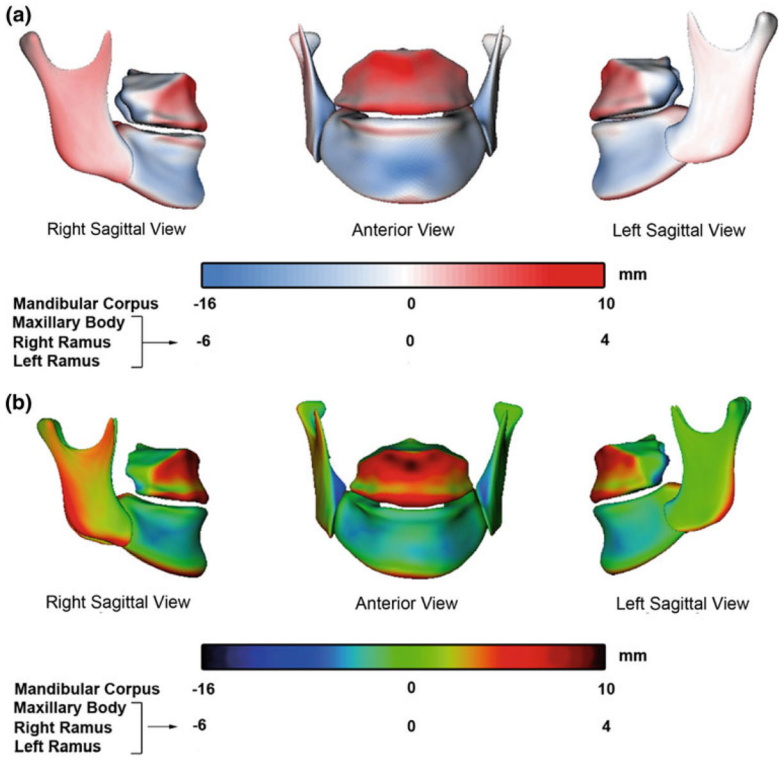

Fig. 5.

Example of a patient for whom mandibular set-back and maxillary advancement were planned, without genioplasty showing color maps visualization of surface distances between pre-surgery and virtually simulated surgery models. **a** Quantification of surgical displacements with corresponding surface distances (SPHARM-PDM). **b** Quantification of surgical displacements with CP surface distances. Note that the SPHARM-PDM *color maps* detect the marked mandibular setback of close to 16 mm and for such large displacements, CP underestimates the displacements

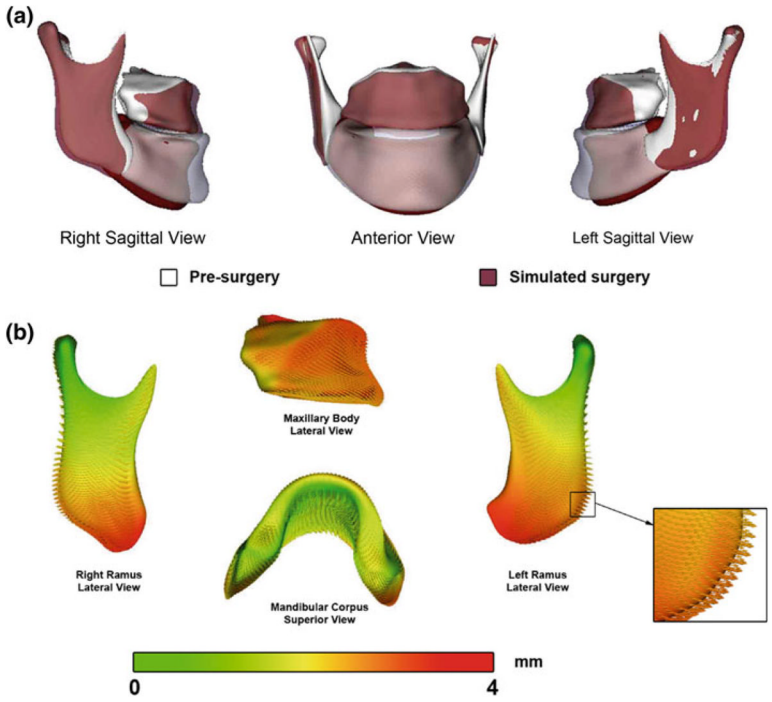

Fig. 6.

Superimposition of pre-surgery and virtually simulated surgery models for the same patient as in Fig. 5. **a** Semi-transparent overlays between pre-surgery and virtually simulated surgery models. **b** For each anatomic region, SPHARM-PDM also provides vector differences that indicate the directionality of displacements. Vector maps are *color-coded* according to the vector magnitude i.e. *red* vectors show big displacements, *green* show little displacements

Table 1

Statistical analysis per type of surgical segment

	Translation in mm			**Rotation in degrees**		
	***X*-plane**	***Y*-plane**	***Z*-plane**	***X*-plane**	***Y*-plane**	***Z*-plane**
Chin						
95% CI	(−0.19, 0.16)	(−1.05, 1)	(−0.87, 0.49)	(−1.69, 1.95)	(−0.23, 0.20)	(−0.46, 0.74)
95% PI	(−0.46, 0.43)	(−2.55, 2.49)	(−1.86, 1.48)	(−4.32, 4.58)	(−0.55, 0.52)	(−1.65, 1.34)
$\bar{d}_j$	−0.01	−0.02	−0.18	0.12	−0.01	0.13
$P(\lvert\bar{d}_{jtra,rot}\rvert < thr)$	0.99	0.75	0.88	0.99	0.99	0.99
Left ramus						
95%*C I*	(−0.03, 0.13)	(−0.25, 0.06)	(−0.07, 0.21)	(−0.68, 0.2)	(−0.04, 0)	(−0.27, 0.06)
$P(\lvert\bar{d}_{jtra,rot}\rvert < thr)$	1	0.99	0.99	1	1	1
Right ramus						
95%*C I*	(−0.23, 0.05)	(−0.23, 0.06)	(−0.06, 0.12)	(−0.06, 0.13)	(−0.2, 0.04)	(−0.06, 0)
95%*P I*	(−0.63, 0.45)	(−0.63, 0.47)	(−0.32, 0.38)	(−0.34, 0.4)	(−0.54, 0.38)	(−0.15, 0.09)
$\bar{d}_j$	−0.08	−0.08	0.02	0.03	−0.08	−0.02
$P(\lvert\bar{d}_{jtra,rot}\rvert < thr)$	0.99	0.99	1	1	1	1
Maxillary body						
95%*C I*	(−0.06, 0)	(0.12,0.43)	(−0.37, 0.16)	(−0.35, 0.43)	(−0.28, 0.28)	(−0.47, −0.06)
95%*P I*	(−0.18, 0.12)	(−0.44, 1)	(−1.34, 1.13)	(−1.83, 1.76)	(−1.31, 1.31)	(−1.21, 0.67)
$\bar{d}_j$	−0.02	0.27	−0.1	0.03	0	−0.27
$P(\lvert\bar{d}_{jtra,rot}\rvert < thr)$	1	0.99	0.99	1	1	1
Mandibular body						
95%*C I*	(−0.14, 0.09)	(−0.25, 0.13)	(−0.28, 0.17)	(−7.75, 0.97)	(−0.71, 0.41)	(−0.84, 0.13)
95%*P I*	(−0.45, 0.4)	(−0.76, 0.63)	(−0.88, 0.77)	(−19.13, 12.35)	(−2.19, 1.89)	(−2.12, 1.4)
$\bar{d}_j$	−0.02	−0.06	−0.05	−3.39	−0.15	−0.35
$P(\lvert\bar{d}_{jtra,rot}\rvert < thr)$	0.99	0.99	0.99	0.97	1	1

Displayed results show very high probability (ranging 0.99–1, except for Chin segment in the *Y*-plane of translation) that the difference between the real measurements and SPHARM measurements was less than 5 degrees of rotation and 0.5 mm of translation. The 95% prediction PI intervals (PIs) and confidence intervals (CI) contained the hyphotesized mean

Int J Comput Assist Radiol Surg. Author manuscript; available in PMC 2012 September 1.

Table 2

Statistical analysis of all surgical segments

	Translation in mm			Rotation in degrees		
	***X*-plane**	***Y*-plane**	***Z*-plane**	***X*-plane**	***Y*-plane**	***Z*-plane**
All segments						
95% CI	(−0.05, 0.01)	(−0.05, 0.15)	(−0.11,0.05)	(−1.27, 0.14)	(−0.19, 0.14)	(−0.30, 0.01)
95% PI	(−0.19, 0.15)	(−0.43, 0.53)	(−0.43, 0.36)	(−3.82, 2.69)	(−0.8, 0.75)	(−0.86,0.57)
$\bar{d}_j$	−0.01	0.05	−0.03	−0.56	−0.02	−0.14
$P(\lvert\bar{d}_{jtra,rot}\rvert < thr)$	1	1	1	1	1	1

Displayed results show very high probability (1 for all planes of rotation and translation) that the difference between the real measurements and SPHARM measurements was less than 5 degrees of rotation and 0.5 mm of translation. PI intervals and CI intervals contained the hyphotesized mean